resolution Imaging Spectroradiometer) sensor on the Earth Observing System satellite. MODIS provides an enhanced remote-sensing capability (*33*) that will enable precise monitoring not only of the interaction of smoke with clouds but also of the spatial distribution of precipitable water vapor, presently available only from sparse radiosonde data. At that time, testing the hypothesized impact of water vapor on the smoke-cloud interaction will be possible.

REFERENCES AND NOTES

1. A. Jones, D. L. Roberts, A. Slingo, *Nature* **370**, 450 (1994).
2. J. E. Penner, R. E. Dickinson, C. A. O'Neill, *Science* **256**, 1432 (1992).
3. J. Hansen, M. Sato, A. Lacis, R. Ruedy, *Philos. Trans. R. Soc. London Ser. B* **352**, 231 (1997).
4. S. E. Schwartz *et al.*, in *Aerosol Forcing of Climate*, R. J. Charlson and J. Heintzenberg, Eds. (Wiley, Chichester, UK, 1995), pp. 251–280.
5. P. J. Crutzen and M. O. Andreae, *Science* **250**, 1669 (1990); A. W. Setzer and M. C. Pereira, *Ambio* **20**, 19 (1991); P. Artaxo, F. Gerab, M. A. Yamasoe, J. V. Martins, *J. Geophys. Res.* **99**, 22857 (1994); W. M. Hao and M.-H. Liu, *Global Biogeochem. Cycles* **8**, 495 (1994).
6. Y. J. Kaufman *et al.*, *J. Geophys. Res.* **97**, 14581 (1992).
7. P. V. Hobbs, J. S. Reid, R. A. Kotchenruther, R. J. Ferek, R. Weiss, *Science* **275**, 1776 (1997).
8. S. Twomey, M. Piepgrass, T. L. Wolfe, *Tellus* **36b**, 356 (1984); P. V. Hobbs, in *Aerosol-Cloud-Climate Interactions*, P. V. Hobbs, Ed. (Academic Press, New York, 1993), p. 33.
9. L. F. Radke *et al.*, *Global Biomass Burning* (MIT Press, Cambridge, MA, 1991), p. 209.
10. C. Liousse, C. Devaux, F. Dulac, H. Cachier, *J. Atmos. Chem.* **22**, 1 (1995).
11. J. Warner and S. Twomey, *J. Atmos. Sci.* **24**, 704 (1967); P. V. Hobbs and L. F. Radke, *Science* **163**, 279 (1969); J. G. Hudson, J. Hallett, C. F. Rogers, *J. Geophys. Res.* **96**, 10847 (1991).
12. D. A. Hegg, L. F. Radke, P. V. Hobbs, *J. Geophys. Res.* **96**, 18727 (1991); W. R. Leaitch, J. W. Strapp, G. A. Isaac, J. G. Hudson, *Tellus* **38B**, 328 (1986).
13. Y. J. Kaufman and T. Nakajima, *J. Appl. Meteorol. Squires Spec. Issue* **32**, 729 (1993).
14. L. A. Remer, Y. J. Kaufman, B. N. Holben, *Global Biomass Burning*, J. Levin, Ed. (MIT Press, Cambridge, MA, 1996), p. 519.
15. M. O. Andreae *et al.*, *J. Geophys. Res.* **99D**, 12793 (1994); P. Artaxo, F. Gerab, M. A. Yamasoe, J. V. Martins, in (*14*), p. 519.
16. P. Le Canut *et al.*, *J. Geophys. Res.* **101**, 23615 (1996); B. E. Anderson *et al.*, *ibid.*, p. 24117.
17. H. Cachier, M. P. Bremond, P. Buat-Ménard, *Nature* **340**, 371 (1989).
18. C. Liousse *et al.*, *J. Chem.* **22**, 1 (1996).
19. J. A. Coakley Jr. and R. Davies, *J. Atmos. Sci.* **43**, 1025 (1986); J. A. Coakley Jr., *Tellus* **43B**, 420 (1991).
20. S. Platnick and S. Twomey, *J. Appl. Meteorol.* **33**, 334 (1994); S. Platnick and F. P. J. Valero, *J. Atmos. Sci.* **52**, 2985 (1995).
21. Apparent temperature is derived from the radiance at 11 μm measured by the satellite, T_{11}. It is lower by a few degrees kelvin than the actual temperature, because it is derived assuming that the cloud top is a black body and ignoring effects of the atmosphere above the cloud.
22. The 0.64-μm channel was corrected for sensor degradation [Y. J. Kaufman and B. N. Holben, *Int. J. Remote Sens.* **14**, 21 (1993); N. Che and J. C. Price, *Remote Sens. Environ.* **41**, 19 (1992)]. The on-board black bodies that emit thermal radiation in fixed temperatures are used to calibrate the 3.7- and 11-μm channels. The cloud reflectance at 3.7 μm, ρ_{c4}, was derived by subtracting the emissive part at 3.7 μm computed with T_{11} and correcting for attenuation and emission by water vapor derived from radiosonde data. Profiles of water vapor measured from radiosonde were obtained from the National Center for Atmospheric Research (obtained from D. Joseph, personal communication). In the analysis, the emissivity was assumed to be 1.0 at 11 μm and $1 - \rho_{c4}$ at 3.75 μm, because clouds selected by Eq. 1 are not transparent in these infrared channels (*13*). A sensitivity and validation study (*20*) indicates accuracy of the cloud droplet size for a similar method of ±2 μm and a precision that is better than that. τ_s is derived from the satellite-measured radiance over cloud-free, shadow-free pixels with dark vegetation cover (*13*, *34*) by means of a smoke optical model (*14*). Similar procedures applied to satellite data resulted in an uncertainty of $\Delta\tau_s \pm 0.1$ (*35*). For high optical thickness, an error of 20 to 30% is expected from uncertainty in the smoke-scattering phase function and single-scattering albedo.
23. A. Arking and J. D. Childs, *J. Climate. Appl. Meteorol.* **24**, 322 (1985).
24. W. R. Leaitch, G. A. Isaac, J. W. Strapp, C. M. Banic, H. A. Wiebe, *J. Geophys. Res.* **97**, 2463 (1992).
25. S. E. Schwartz and A. Slingo, *NATO ASI Series* **135**, 192 (1996).
26. S. A. Twomey, *J. Atmos. Sci.* **34**, 1149 (1977).
27. O. Boucher and T. L. Anderson, *J. Geophys. Res.* **100**, 26117 (1995).
28. T. C. Novakov, C. Rivera-Carpio, J. E. Penner, C. F. Rogers, *Tellus* **46B**, 132 (1994).
29. W. R. Leaitch *et al.*, *J. Geophys. Res.* **101**, 29103 (1996).
30. P. J. Crutzen *et al.*, *J. Atmos. Chem.* **2**, 233 (1985). For effects of convections see R. R. Dickerson *et al.*, *Science* **235**, 18473 (1987); V. W. J. H. Kirchhoff and E. V. A. Marinho, *Atmos. Environ.* **28**, 69 (1994); K. E. Pickering *et al.*, *J. Geophys. Res.* **101**, 23993 (1996).
31. The value determined by Penner *et al.* (*2*) of the global average indirect forcing by smoke could be an overestimate because (i) the study assumes a global homogeneous spatial distribution of the smoke aerosol in the presence of nonlinearity of the smoke effect; (ii) it neglects the presently observed low forcing for low availability of precipitable water vapor; and (iii) it neglects the production of smoke in the dry season with low cloud fraction.
32. T. R. Karl, R. W. Knight, G. Kukla, J. Gavin, in (*4*), pp. 363–384.
33. M. D. King, Y. J. Kaufman, P. Menzel, D. Tanre, *IEEE J. Geosci. Remote Sens.* **30**, 2 (1992); V. V. Salomonson, W. L. Barnes, P. W. Maymon, H. E. Montgomery, H. Ostrow, *ibid.* **27**, 145 (1989).
34. Y. J. Kaufman and C. Sendra, in *Aerosols and Climate*, P. V. Hobbs and M. P. McCormick, Eds. (Deepak, Hampton, VA, 1988), p. 51; B. N. Holben, E. Vermote, Y. J. Kaufman, D. Tanré, V. Kalb, *IEEE Trans. Geosci. Remote Sens.* **30**, 212 (1992); Y. J. Kaufman, in (*4*), p. 298.
35. R. S. Fraser, Y. J. Kaufman, R. L. Mahoney, *Atmos. Environ.* **18**, 2577 (1984); P. A. Durkee, D. R. Jensen, E. E. Hindman, T. H. Vonder Haar, *J. Geophys. Res.* **91**, 4063 (1986); P. A. Durkee, F. Pfeil, E. Frost, R. Shema, *Atmos. Environ.* **25a**, 2457 (1991); E. F. Vermote *et al.*, Special issue on Remote Sensing of Aerosol, *J. Geophys. Res.* **102**, 17131 (1997).

36. The satellite data were analyzed by S. Mattoo. The cloud detection was developed by M. Lawrence during a summer fellowship program at NASA Goddard Space Flight Center. We thank J. Tucker for assistance with AVHRR data and acknowledge valuable comments from O. Boucher, P. V. Hobbs, Y. Joseph, M. D. King, Z. Levin, J. E. Penner, S. Platnick, L. A. Remer, and D. Tanré.

29 May 1997; accepted 5 August 1997

Explosive Basaltic Volcanism from Cerro Negro Volcano: Influence of Volatiles on Eruptive Style

Kurt Roggensack,* Richard L. Hervig,† Steven B. McKnight,‡ Stanley N. Williams

The 1992 and 1995 basaltic eruptions of Cerro Negro volcano, Nicaragua, had contrasting eruptive styles. Although they were nearly identical in composition, the 1992 eruption was explosive, producing a 7-kilometer-high sustained ash column, whereas the 1995 eruption was essentially effusive. The differences in water and carbon dioxide contents of melt inclusions from the two eruptions define minimum saturation pressures and show how decompression of initially similar magmas influences eruptive style. Before eruption, the explosive 1992 magma retained water and carbon dioxide while ascending to a moderate crustal level (about 6 kilometers), whereas the nonexplosive 1995 magma lost all carbon dioxide by degassing during ascent to shallow crustal levels (about 1 to 2 kilometers).

Exsolution of water and carbon dioxide from erupting magmas provides the energy for explosive volcanism (*1*), but it has been difficult to correlate preeruptive volatile contents of magmas with eruption style (*2*) because factors such as conduit geometry, magma viscosity, and degassing history may also affect the explosivity of eruptions. Most earlier work has concentrated on silicic rather than basaltic explosive eruptions. Here, we contrast two recent eruptions of basaltic magma from the Cerro Negro volcano, Nicaragua, that show different eruptive styles, despite a common composition and vent geometry.

Cerro Negro is a small (~250 m high) basaltic volcano (Fig. 1) that has frequent but highly variable activity. The volcano's two most recent events highlight these differences. The April 1992 eruption, the first since 1971, was particularly energetic for a

Department of Geology, Box 871404, Arizona State University, Tempe, AZ 85287–1404, USA.

*To whom correspondence should be addressed.
†Also at Center for Solid State Science, Box 871704, Arizona State University, Tempe, AZ 85287–1704, USA.
‡Present address: Friends Seminary, 222 East 16 Street, New York, NY 10003, USA.

Table 1. Major element analyses of eruptives from Cerro Negro volcano. All analyses are given in weight % oxide normalized to 100% on a volatile-free basis; the total iron is reported as FeO. MI and MG analyses were determined by an electron microprobe with a 10- to 20-μm beam, 15-keV accelerating voltage, and 10-nA beam current. Most analyses represent a single analysis point. Sodium was counted first in the analysis cycle, and on-peak counting times were limited to 10 s to minimize Na loss. The typical percentage standard deviation based on counting statistics is as follows: SiO_2, 1; TiO_2, 4; Al_2O_3, 1.5; FeO, 4; MnO, 25; MgO, 5; CaO, 2; Na_2O, 4; K_2O, 5; P_2O_5, 25; S, 17; and Cl, 15. Bulk rock analyses were determined by x-ray fluorescence on fused lithium tetraborate disks. P14(avg.) represents the average of four separate lapilli analyses. Three lava analyses from 1995 eruption are identical within analytical error. The phenocryst assemblage was dominated by calcic plagioclase (An_{74-93}) with lesser amounts of clinopyroxene ($En_{44}Wo_{48}Fs_8$–$En_{41}Wo_{41}Fs_{18}$), olivine (Fo_{71-83}), and magnetite. The crystal abundances of 1992 and 1995 eruptives are ~40 and 43% (by volume), respectively. The dashes indicate that values were not determined.

Sample	Year	Type	SiO_2	TiO_2	Al_2O_3	FeO	MnO	MgO	CaO	Na_2O	K_2O	P_2O_5	S	Cl	Orig. total
P14(avg.)	1992	Bulk	50.12	0.78	19.03	10.17	0.19	5.17	11.75	2.20	0.48	0.11	–	–	98.93
P14-db	1992	Bulk	48.84	0.74	18.02	10.11	0.19	6.07	11.79	2.02	0.43	0.10	–	–	98.31
95L1	1995	Bulk	50.17	0.77	17.99	10.14	0.20	6.46	11.44	2.25	0.46	0.11	–	–	98.93
2H	1992	MI	48.64	0.71	18.35	10.42	0.17	6.23	13.17	1.90	0.34	0.07	0.08	0.07	91.45
7B1a	1992	MI	50.05	0.91	16.39	12.30	0.20	6.07	11.14	2.44	0.47	0.02	0.08	0.08	95.53
5M	1992	MI	52.15	1.07	16.49	11.47	0.21	5.49	9.80	2.67	0.55	0.11	0.00	0.12	94.41
4a-2	1995	MI	48.11	0.71	18.59	10.14	0.15	6.96	12.95	2.11	0.19	0.09	0.13	0.07	95.05
4a-4c	1995	MI	52.19	1.00	15.74	10.84	0.22	5.70	11.11	2.47	0.56	0.17	0.06	0.11	95.24
4a-11	1995	MI	51.15	1.01	16.06	12.97	0.26	5.39	9.54	2.79	0.66	0.17	0.03	0.15	96.09
7B1	1992	MG	54.49	1.44	14.43	14.58	0.27	3.46	9.44	2.91	0.85	0.18	–	–	95.20
4A	1995	MG	55.66	1.54	12.80	14.18	0.25	3.51	8.30	2.62	0.87	0.25	–	–	98.31

basaltic eruption (3) and produced a high (~7 km) sustained ash column (4). In contrast, the 1995 eruption began with small discrete ash explosions (<2 km in height) from May to August. Eruptive activity resumed in November with lava emission and ash explosions of varying intensity and frequency (columns as high as 2.5 km) (5, 6).

Despite differences in eruptive style, the 1992 and 1995 eruptions were similar in composition (Table 1) (7). The compositions of melt inclusions (MIs) trapped in growing olivine (Fo_{71-83}) crystals varied widely in both eruptions (for example, K_2O values varied from 0.15 to 0.73 weight %). Partitioning of Fe and Mg between olivine and trapped melt (8) indicates that less than 3% of the inclusion crystallized after the melt was trapped. Careful inspection of crystals before polishing eliminated cracked MIs, thus minimizing the possibility of volatile leakage. We took these samples to represent magma present earlier in time, yielding snapshots of the evolution of the magma feeding each eruption. Analyses of matrix glass (MG) showed slightly higher K_2O values [0.85 and 0.87 weight % (Table 1)] than the most evolved MI, suggesting that the variation in MI composition can be explained by fractional crystallization.

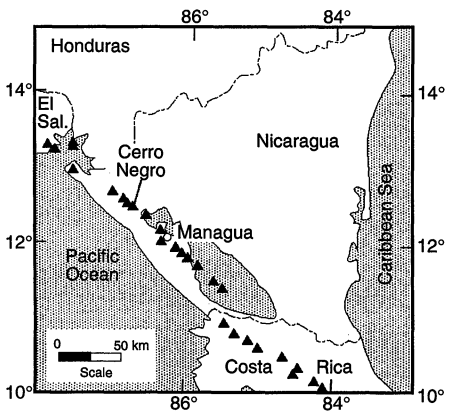

Fig. 1. Location map of the Cerro Negro volcano (24).

The volatile contents of the MIs from the 1992 and 1995 eruptions were different, as were their calculated saturation pressures (Fig. 2) (9). MIs with high volatile contents would be saturated with a CO_2–H_2O gas at pressures from 0.3 to >0.5 GPa (depths of ~10 to 15 km). These MIs showed relatively primitive compositions (high MgO and low K_2O contents) and quite variable trace element abundances (10). Volatile contents for low-pressure MIs (<0.3 GPa) from the two eruptions varied systematically with the degree of crystal fractionation [for example, K_2O content (Fig. 3)] (11). Although similar degrees of crystallization (~50%) were represented by both eruptions, the low volatile contents in the

Table 2. Melt inclusion water and CO_2 contents determined by infrared spectroscopy (22) and their corresponding equilibrium vapor saturation pressures (9). The analytical error is less than 10% for H_2O. The analytical error for CO_2 increases from ~15% at >400 ppm to ~100% at ~50 ppm. Below detection limit, b.d.l.

Sample	Eruption year	K_2O (weight %)	H_2O (weight %)	CO_2 (ppm)	Pressure (GPa)
2B	1992	0.14	6.08	1039	0.62
2D	1992	0.17	5.36	499	0.44
2J	1992	0.20	5.16	674	0.44
1H	1992	0.24	5.27	951	0.51
2Ka	1992	0.24	3.21	388	0.20
2H	1992	0.34	3.82	902	0.35
7B1-1	1992	0.47	4.23	311	0.27
2Kb	1992	0.48	2.93	145	0.12
2I	1992	0.51	4.20	267	0.26
5M	1992	0.55	3.75	342	0.23
2F	1992	0.58	4.70	b.d.l.	0.24
7C2*	1992	0.60	4.28	106	0.22
5B*	1992	0.61	4.00	185	0.22
5K	1992	0.67	4.22	b.d.l.	0.19
4a-2	1995	0.19	4.23	651	0.34
4a-4a	1995	0.29	3.09	373	0.18
4a-10b	1995	0.29	3.16	67	0.12
4a-5a	1995	0.31	5.15	320	0.36
4a-3b*	1995	0.35	4.08	10	0.18
4a-9	1995	0.43	1.18	b.d.l.	0.01
4a-8	1995	0.48	3.07	b.d.l.	0.09
4a-10a	1995	0.49	2.95	64	0.10
4a-4c	1995	0.56	3.37	b.d.l.	0.12
4a-11	1995	0.66	2.80	b.d.l.	0.08

*MI with high TiO_2 (23).

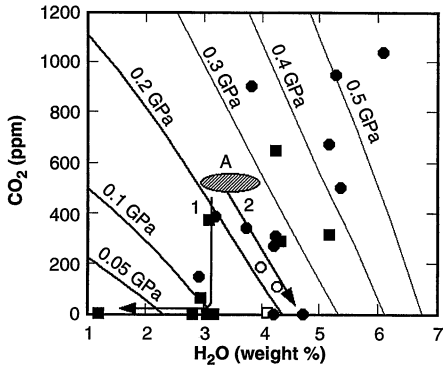

Fig. 2. CO_2 and H_2O variation in olivine MIs from the 1992 (filled circles) and 1995 (filled squares) eruptions. Open symbols indicate MIs with high TiO_2 (*23*). Lines are fluid-saturation isobars (0.05 to 0.5 GPa) (*9*). The arrows show schematic trends for open-system decompression degassing (labeled 1) and fluid-saturated isobaric crystallization (labeled 2). The hatched area (labeled A) shows a possible parent to the 1992 and 1995 low-pressure (<0.3 GPa) MIs.

1995 MIs indicate that they were trapped at shallower depths than the 1992 MIs.

There is growing evidence from MIs (*12*) and experimental work (*13*) that high volatile contents, like those measured at Cerro Negro, are common in basaltic magmas associated with subduction zones. Volatile-rich magmas will begin to degas upon reaching volatile saturation in the crust, and our data indicate that, before the eruption, the 1992 melt did not rise as high in the crust as the 1995 melt. As a result, the 1992 melt evidently retained a greater abundance of volatiles (H_2O and CO_2) and erupted explosively. Several of the 1992 MIs that fall on the low-pressure 1995 trend can be explained as xenocrysts or, more likely, as a small part of the 1992 melt that reached shallow levels before the 1992 eruption.

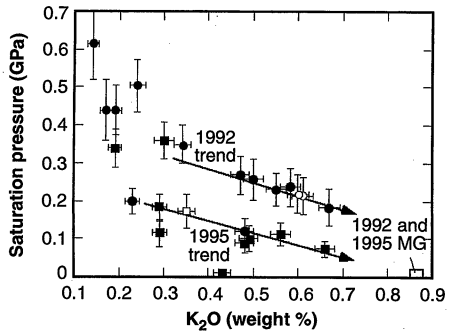

Fig. 3. Correlation of MI fluid-saturation pressures (CO_2 and H_2O) with fractionation index. Symbols are as in Fig. 2. The schematic arrows were drawn visually. The error bars are based on conservative estimates of Fourier transform infrared spectroscopy (FTIR) error (see Table 2) and electron probe counting statistics.

Variations in other parameters linked to eruptive style are small compared with the observed differences in preeruptive volatile contents. For example, the bulk composition and the crystal content [which affects viscosity (*14*)] were similar in the two eruptions (Table 1). Vent geometry (*15*) is unlikely to have varied greatly, because Cerro Negro's cone morphology was unchanged since the 1992 eruption and the vent location has been stable for nearly 150 years (*16*). The basaltic explosive eruptions have not been as destructive or voluminous as silicic plinian eruptions, which tend to destroy their volcanic plumbing systems. Thus, the dominant variable controlling eruptive style is preeruptive volatile content.

Magma rise speed may also affect eruptive style (*17*) and is geologically well constrained. The 1992 event was a sustained explosive eruption (*3*), indicating that magma rose from ~6-km depth at a high rate that prevented bubble coalescence (*17*). Magma rise speed for the 1995 eruption may have been lower, or, more likely, variations in rise speed may have caused the changing character of the eruption.

Extensive studies of mostly effusive eruptions on Hawaii have formed the basis for models of nonexplosive basaltic volcanism (*18*). However, it is clear that explosive basaltic volcanism is also common (*19*). These explosive eruptions are not merely a result of secondary processes (for example, magma interaction with ground water) nor are they exceptionally vigorous nonexplosive activity (that is, fire fountaining). Instead, events such as Cerro Negro's 1992 eruption are truly explosive basaltic volcanism. Our results demonstrate how the decompression history of initially similar magmas can greatly influence basaltic eruption styles (*20*). Our results also identify the importance of volatiles in explosive basaltic volcanism (*21*) and suggest that explosive basaltic eruptions could also occur on other planets.

REFERENCES AND NOTES

1. C. W. Burnham, *Econ. Geol.* **80**, 1515 (1985).
2. C. M. Skirius, J. W. Peterson, A. T. Anderson Jr., *Am. Mineral.* **75**, 1381 (1990); C. R. Bacon, S. Newman, E. Stolper, *ibid.* **77**, 1021 (1992); N. W. Dunbar and R. L. Hervig, *J. Geophys. Res.* **97**, 15129 (1992); *ibid.*, p. 15151.
3. C. B. Connor *et al.*, *Eos* (*Fall Suppl.*) **74**, 640 (1993).
4. C. Gutiérrez *et al.*, *Global Volcanism Net. Bull.* **17** (no. 3), 2 (1992); G. J. Soto *et al.*, *ibid.* (no. 4), p. 7. Attempts to classify explosive basaltic volcanism have highlighted problems with recognition of this class of activity. The high sustained ash column and continuous explosion of the 1992 eruption are like those observed in silicic plinian eruptions. In addition, scoria from the 1992 eruption show none of the textures commonly produced by fire fountaining [G. Heiken, *Geol. Soc. Am. Bull.* **83**, 1961 (1972)].
5. W. Strauch and A. Cruesot-Eon, *Global Volcanism Net. Bull.* **20** (no. 5), 2 (1995); M. Navarro *et al.*, *ibid.* **20** (no. 9), 9 (1995); W. Strauch *et al.*, *ibid.* **20** (no. 11/12), 2 (1995).
6. Eruptive volumes (dense rock equivalent) for the 1992 and 1995 eruptions are similar: 0.01 km^3 and 0.008 km^3, respectively [B. Hill, personal communication; B. Hill *et al.*, in *Volcanic Activity and the Environment, IAVCEI Abstracts*, International Association of Volcanology and Chemistry of the Earth's Interior, Puerto Vallarta, Mexico, 19 to 24 January 1997 (Unidad Editorial, Guadalajara, Mexico, 1997), p. 38]. The 1992 eruption lasted 5 days, and most of the ash fell during the first 18 hours (*3*). The main phase of the 1995 eruption began in November and lasted roughly 2.5 weeks (*5*).
7. Cerro Negro eruptives are crystal-rich and sometimes show evidence of crystal accumulation [J. A. Walker and M. J. Carr, *Geol. Soc. Am. Bull.* **97**, 1156 (1986)]. In addition, the inherent nature of small-volume eruptions preserves greater heterogeneity [W. G. Melson *et al.*, *J. Volcanol. Geotherm. Res.* **41**, 97 (1990)] and probably greater detail of the magma system. The most magnesian 1992 lapilli sample closely approaches the 1995 lava, whereas the average composition of four 1992 lapilli is slightly less magnesian than the 1995 lavas. The similarity of MG compositions further suggests that the 1992 and 1995 magmas were nearly compositionally identical. Olivine crystals (Fo_{71-83}) in ash and lava are euhedral, vary widely in size (0.7- to 3.5-mm maximum dimension), and commonly feature small glass reentrants along their margins.
8. P. L. Roeder and R. F. Emslie, *Contrib. Mineral. Petrol.* **29**, 27 (1970).
9. C. W. Burnham, in *Volatiles in Magmas*, vol. 30 of *Reviews in Mineralogy*, M. R. Carroll and J. R. Holloway, Eds. (Mineralogical Society of America, Washington, DC, 1994), pp. 123–129; J. R. Holloway and J. G. Blank, in *Volatiles in Magmas*, vol. 30 of *Reviews in Mineralogy*, M. R. Carroll and J. R. Holloway, Eds. (Mineralogical Society of America, Washington, DC, 1994), pp. 187–230.
10. K. Roggensack *et al.*, in preparation.
11. We focused on low-pressure MIs (<0.3 GPa) because they show a correlation between composition and saturation pressure that extends upward to the point at which the magma was erupted. The range of K_2O variation along the systematic array is similar for 1992 and 1995 MIs (~0.30 to 0.65 weight %) and represents roughly 50% crystallization. It is important that the low-pressure (<0.3 GPa) MIs in the 1992 and 1995 eruptions could be derived from a melt of similar major element composition and volatile content (Fig. 2). For example, decompression degassing and intervals of fluid-saturated crystallization of a melt containing roughly 3 to 4 weight % H_2O and ~500 parts per million CO_2 could produce the 1992 and 1995 low-pressure MIs.
12. T. W. Sisson and G. D. Layne, *Earth Planet. Sci. Lett.* **117**, 619 (1993); A. V. Sobolev and M. Chaussidon, *ibid.* **137**, 45 (1996).
13. G. A. Gaetani, T. L. Grove, W. B. Bryan, *Nature* **365**, 332 (1993); T. W. Sisson and T. L. Grove, *Contrib. Mineral. Petrol.* **113**, 167 (1993).
14. H. R. Shaw, D. L. Peck, T. L. Wright, R. Okamura, *Am. J. Sci.* **266**, 225 (1968).
15. R. S. J. Sparks, *J. Volcanol. Geotherm. Res.* **3**, 1 (1978); L. Wilson and J. W. Head III, *J. Geophys. Res.* **86**, 2971 (1981); S. J. Blake, *ibid.* **89**, 8237 (1984); C. Jaupart and C. J. Allégre, *Earth Planet. Sci. Lett.* **102**, 413 (1991).
16. S. B. McKnight, thesis, Arizona State University, Tempe, AZ (1995).
17. Models of explosive eruptions require that gas remain dispersed in the parent magma before fragmentation, and for low-viscosity magmas, rapid magma rise speeds are required [L. Wilson, *J. Volcanol. Geotherm. Res.* **8**, 297 (1980)].
18. J. W. Head III and L. Wilson, *ibid.* **37**, 261 (1989); S. Vergniolle and C. Jaupart, *J. Geophys. Res.* **95**, 2793 (1990); E. A. Parfitt, L. Wilson, C. A. Neal, *Bull Volcanol.* **57**, 440 (1995).
19. Examples of explosive basaltic volcanism include Masaya, Nicaragua [S. N. Williams, *Geology* **11**, 211 (1983)], Ambrym, Vanuatu [C. Robin, J. P. Eissen, M. Monzier, *J. Volcanol. Geotherm. Res.* **55**, 225 (1993)], Tolbachik, Kamchatka [S. A. Fedotov and Ye. K. Markhinin, Eds., *The Great Tolbachik Fissure*

Eruption (Cambridge Univ. Press, New York, 1983)], and Sumisu Rift, Japan [J. Gill *et al.*, *Science* **248**, 1214 (1990)].
20. High water contents (*12*) were also reported for the explosive 1974 basaltic andesite eruption of Fuego {vulcanian [W. I. Rose Jr., A. T. Anderson Jr., L. G. Woodruff, S. B. Bonis, *J. Volcanol. Geotherm. Res.* **4**, 3 (1978)]}. Subsequent MI analyses (K. Roggensack, unpublished data) have shown that the Fuego magma also contained considerable CO_2.
21. Another implication of the trend of decreasing saturation pressure with increasing fractionation (higher K_2O) is that these eruptions were not fed by stable shallow crustal-level magma chambers. Instead, the magma was moving upward as it fractionated, and this movement probably prevented settling of MIs that were formed earlier (that is, MIs with high saturation pressures). Also, despite the systematic variation shown in Fig. 3, many MIs do not follow a simple paragenetic sequence, suggesting that the magma was transported by a network of dikes rather than a single dike.
22. The extinction coefficient for CO_3^{2-} (375 l/mol·cm) is from G. Fine and E. Stolper [*Earth Planet. Sci. Lett.* **76**, 263 (1986)]. The extinction coefficients for H species (0.62 at band 5200 cm^{-1} and 0.67 at band 4500 cm^{-1}) are from J. E. Dixon, E. M. Stolper, and J. R. Holloway [*J. Petrol.* **36**, 1607 (1995)]. The extinction coefficient for total water (63 at band 3550 cm^{-1}) is from J. E. Dixon, E. Stolper, and J. R. Delaney [*Earth Planet. Sci. Lett.* **90**, 87 (1988)]. Basalt glass density is assumed to be constant at 2800 g/liter. Wafer thickness was measured optically by viewing crystal edgewise.
23. M. J. Carr, M. D. Feigenson, E. A. Bennett, *Contrib. Mineral. Petrol.* **105**, 369 (1990); J. A. Walker, M. J. Carr, M. D. Feigenson, R. I. Kalamarides, *J. Petrol.* **31**, 1141 (1990); W. P. Leeman, M. J. Carr, J. D. Morris, *Geochim. Cosmochim. Acta* **58**, 149 (1994).
24. T. Simkin and L. Siebert, *Volcanoes of the World* (Geoscience, Tucson, AZ, ed. 2, 1994).
25. We thank the people of Instituto Nicaraguense de Estudios Territorales and particularly M. Navarro for logistical support and help in the field, B. Hill for providing additional samples, J. Lowenstern for access and help with the FTIR, J. Clark for analytical assistance with electron microprobe (instrument support NSF grant EAR 8408163), S. Selkirk for help with figure preparation, and J. E. Dixon and an anonymous reviewer for constructive comments. Partial financial support was provided by NSF, Arizona State University, and the United Nations.

10 June 1997; accepted 11 August 1997

Measurements of the Cretaceous Paleolatitude of Vancouver Island: Consistent with the Baja–British Columbia Hypothesis

Peter D. Ward,* José M. Hurtado, Joseph L. Kirschvink, Kenneth L. Verosub

A previously unsampled outcrop of gently dipping or flat-lying Upper Cretaceous sedimentary strata in the Vancouver Island region, which contains unaltered aragonitic mollusk fossils, yielded a stable remanent magnetization that is biostratigraphically consistent with Cretaceous magnetochrons 33R, 33N, and 32R. These results, characterized by shallow inclinations, indicate an Upper Cretaceous paleolatitude of about 25 ± 3 degrees north, which is equivalent to that of modern-day Baja California. These findings are consistent with the Baja–British Columbia hypothesis, which puts the Insular Superterrane well south of the Oregon-California border in the Late Cretaceous.

The Cordillera of western North America is composed of an amalgamation of tectonic terranes, which were accreted at various times onto the stable North American continent (Fig. 1). The accretional history of the Insular Superterrane (*1*), which is composed of the northern Cascades of Washington State, the Coast Ranges of western British Columbia, Vancouver Island, the Queen Charlotte Islands, and a large region extending from southeastern Alaska to the Wrangel Mountains in northern Alaska, is currently in dispute. Two conflicting and mutually exclusive hypotheses are favored (*2*). The first hypothesis suggests that the Insular Superterrane lay north of the Franciscan-Sierran convergent plate boundary in California during most, if not all, of the Cretaceous period (*3*). The second hypothesis is that all of the Insular Superterrane north of latitude 49°N and up to 58°N was situated at a minimum of 2400 km south of its present position relative to North America 90 million years ago (Ma) (*4*, *5*, *6*). In this model, the Intermontane Superterrane (Fig. 1) is also expected to be found at least 1000 km south of its modern-day position in the mid-Cretaceous (*2*). This latter hypothesis is called the Baja–British Columbia (BBC) hypothesis because it predicts that, 90 Ma, the Vancouver Island region would have been offshore of present-day Baja California (*2*, *4*).

Evidence that can be used to refute either or both of these hypotheses comes from two main sources: geological and paleomagnetic evidence. Geological evidence includes (i) provenance studies of sediments included within the Insular Superterrane, (ii) the correlation of features found within the Insular Superterrane with similar features found inboard of it, and (iii) features limiting the offset across transcurrent faults to values less than those proposed by the BBC hypothesis. Paleomagnetic evidence relies on the determination of paleolatitudes, which are derived from either igneous or sedimentary rocks. Bedded sedimentary rocks are preferred because the paleohorizontal can be readily observed, eliminating the problem of anomalously low paleolatitudes due to tilting and deformation.

Three sets of paleomagnetic data from the region (Fig. 1), for which tilt corrections have been performed (Mount Stuart batholith, Silverquick conglomerate and volcanics, and the Duke Island ultramafic complex), support the BBC hypothesis (*6*, *7*). Only the Duke Island Complex, however, comes from the Insular Superterrane; the others are from the Coast Mountains orogen and the Intermontane Superterrane. Furthermore, until now, no paleomagnetic data, from either superterrane, have come from well-bedded sedimentary rocks of Cretaceous age in which the original horizontality is unambiguous. Here we present paleomagnetic evidence from well-bedded sedimentary rocks of the Insular Superterrane south of Alaska that is consistent with the BBC hypothesis.

We sampled strata from the Upper Cretaceous Nanaimo Group of Vancouver Island, which had been considered unsuitable for paleomagnetic investigation, because all previous sampling efforts showed a pervasive remagnetization (*8*). However, we located previously unsampled outcrops along the eastern margin of the Nanaimo basin that contain ammonite and inoceramid bivalve fossils composed of unaltered aragonite containing organic macromolecules within concretionary mudstone and siltstone facies. It has been proposed that the presence of such unaltered fossil material is an indication that thermal and chemical remagnetization is minimal to absent (*9*) because (i) the conversion temperature of aragonite to calcite (~100°C) is lower than the blocking temperature of the fine-grained ferromagnetic particles (~400° to 580°C) that record the natural remanent magnetism (NRM) in many clastic sediments and (ii) the presence of organic macromolecules in the fossils indicates that little fluid has passed through the sediment after deposition, retarding di-

P. D. Ward, Department of Geological Sciences, University of Washington, Seattle, WA 98195, USA.
J. M. Hurtado, Department of Earth, Atmospheric, and Planetary Sciences, Massachusetts Institute of Technology, Cambridge, MA 02139, USA.
J. L. Kirschvink, Division of Geological and Planetary Sciences, California Institute of Technology, Pasadena, CA 91125, USA.
K. L. Verosub, Department of Geology, University of California, Davis, CA 95616, USA.
*To whom correspondence should be addressed.